T^* model of the energy distributions of excitations in nonequilibrium superconductors

Jhy-Jiun Chang
Department of Physics, Wayne State University, Detroit, Michigan 48202

Warren Y. Lai
Department of Physics, California Institute of Technology, Pasadena, California 91125

D. J. Scalapino
Department of Physics, University of California, Santa Barbara, California 93106

(Received 26 December 1978)

The coupled set of nonlinear kinetic Boltzmann equations governing the distributions of quasiparticles and phonons in a driven superconductor has been numerically solved. When the coupling between the superconductor and the thermal bath is weak, we find that the numerical solutions are well approximated by an extension of Parker's T^* model. This model leads to simple analytic forms in which the quasiparticle distribution is given by a Fermi function at temperature T^*, and the phonon distribution is a weighted average of Bose distributions at temperatures T^* and the ambient bath temperature T_a.

In order to determine the energy distributions of quasiparticles and phonons in driven superconductors, we have numerically solved the coupled kinetic equations for a variety of external drives.[1] When there is strong thermal coupling between the superconductor and the substrate, the distributions show specific structure associated with the particular drive. However, when there is relatively weak thermal coupling between the superconductor and the temperature bath, we find that our numerical results can be reasonably approximated by a straightforward extension of Parker's T^* model.[2] Here we discuss this extension and compare the numerical solutions with the analytic forms of this extended T^* model.

In these calculations the coupling of the superconductor to the thermal bath is characterized by a phonon escape time τ_{es}. A useful measure of the thermal coupling is the ratio of τ_{es} to the zero-temperature pair-breaking lifetime τ_0^{ph} of a phonon of energy $2\Delta_0$. Values of τ_0^{ph} for various metals obtained from tunneling data are given in Ref. 3. For large values of the ratio τ_{es}/τ_0^{ph}, phonons with energy greater than twice the gap will tend to be trapped by the quasiparticles, alternatively breaking pairs and being reemitted as quasiparticles recombine. Parker suggested that under these conditions a useful theory could be constructed based on a modified heating model in which the strongly coupled system consisting of the phonons with energy greater than 2Δ and the quasiparticles would be characterized by a temperature T^*, while the phonons with less energy than 2Δ would be characterized by the ambient bath temperature T_a.

The solid line in Fig. 1(a) shows the quasiparticle distribution obtained from a numerical solution of the coupled kinetic equations, Eqs. (7) and (8), given in Ref. 1. Here the external drive was tunnel injection at a bias voltage $2\Delta_0/e$ and with a tunneling coupling[4] $A = 0.01$. The ambient temperature was $0.5\ T_c$ and $\tau_{es}/\tau_0^{ph} = 20$. Under these conditions the gap Δ in the nonequilibrium state was equal to $0.66\ \Delta_0$ so that eV was well above the injection threshold. From the BCS equation relating $\Delta(T)$ to T, it follows that a gap of $0.66\ \Delta_0$ implies a value for T^* of $0.84\ T_c$. The dashed line in Fig. 1(a) shows a Fermi function with temperature $T^* = 0.84\ T_c$. While this fails to pick up the small structure at the injection edge $2\Delta_0 - \Delta$, it clearly provides an excellent one-parameter fit.

The solid curve in Fig. 1(b) shows the numerical results for the phonon spectrum $(\Omega/\Delta)^2 n(\Omega)$ obtained from the full kinetic equations of Ref. 1. Parker's model gives a phonon distribution set by the usual Bose function $n(\Omega, T^*)$ for $\Omega > 2\Delta$ and $n(\Omega, T_a)$ for $\Omega < 2\Delta$. Using this, the phonon spectrum $(\Omega/\Delta_0)^2 n(\Omega, T^*)$ is plotted as the dash-dot curve in Fig. 1(b) and gives a reasonable fit for $\Omega > 2\Delta$ but fails for $\Omega < 2\Delta$.

Now, it turns out that if we take the quasiparticle distribution to have the form of a Fermi distribution at a modified temperature T^*, it is straightforward to solve the kinetic equation, Eq. (8) of Ref. 1, for the phonon distribution.[5] For the present tunneling case,

in which there is no external phonon source driving the superconductor, this solution is

$$n(\Omega)=\begin{cases}\dfrac{\tau_s^{-1}(\Omega,T^*)n(\Omega,T^*)+\tau_{es}^{-1}n(\Omega,T_a)}{\tau_s^{-1}(\Omega,T^*)+\tau_{es}^{-1}}, & 2\Delta>\Omega>0\ ,\\ \dfrac{[\tau_s^{-1}(\Omega,T^*)+\tau_B^{-1}(\Omega,T^*)]n(\Omega,T^*)+\tau_{es}^{-1}n(\Omega,T_a)}{\tau_s^{-1}(\Omega,T^*)+\tau_B^{-1}(\Omega,T^*)+\tau_{es}^{-1}}, & \Omega>2\Delta\ ,\end{cases} \tag{1}$$

with n the usual Bose function and $\tau_s(\Omega,T^*)$ and $\tau_B(\Omega,T^*)$ the scattering and pair-breaking lifetimes, respectively, for a phonon of energy Ω in a superconductor at temperature T^*.

$$\tau_s^{-1}(\Omega,T^*)=\frac{2}{\pi\tau_0^{ph}\Delta_0}\int_{\Delta(T^*)}^{\infty}dE\,\rho(E)\rho(E+\Omega)\left[1-\frac{\Delta^2(T^*)}{E(E+\Omega)}\right][f(E,T^*)-f(E+\Omega,T^*)]\ ,$$

$$\tau_B^{-1}(\Omega,T^*)=\frac{1}{\pi\tau_0^{ph}\Delta_0}\int_{\Delta(T^*)}^{\infty}dE\,\rho(E)\rho(\Omega-E)\left[1+\frac{\Delta^2(T^*)}{E(\Omega-E)}\right][1-f(E,T^*)-f(\Omega-E,T^*)]\ . \tag{2}$$

Here $\rho(E)$ is the usual BCS density of states.

From Eq. (1) we see that if the quasiparticles have a T^* Fermi distribution, the phonon distribution is simply given by a weighted average of Bose factors at temperatures T^* and T_a. Since we have assumed $\tau_{es}\gg\tau_0^{ph}$, which implies that $\tau_{es}\gg\tau_B$, $n(\Omega,T^*)$ provides a reasonable approximation for $\Omega>2\Delta$. However, for $\Omega<2\Delta$ it is the scattering time τ_s which must be compared with τ_{es}. If $\tau_{es}\ll\tau_s$, then Eq. (1) gives Parker's result $n(\Omega,T_a)$ for $\Omega<2\Delta$. However, if $\tau_{es}\gtrsim\tau_s$, then there will be a significant weight of the $n(\Omega,T^*)$ distribution altering the Parker result. The form for $n(\Omega)$ given by Eq. (1) takes the interplay of τ_s, τ_B, and τ_{es} into account and gives the actual $n(\Omega)$ provided $f(E)$ is a Fermi distribution characterized by a temperature T^*.

The extended T^* model result for the phonon spectrum $(\Omega/\Delta_0)^2n(\Omega)$ obtained from Eqs. (1) and (2) is plotted as the dashed curve in Fig. 1(b). This curve provides a significantly better fit to the numerical

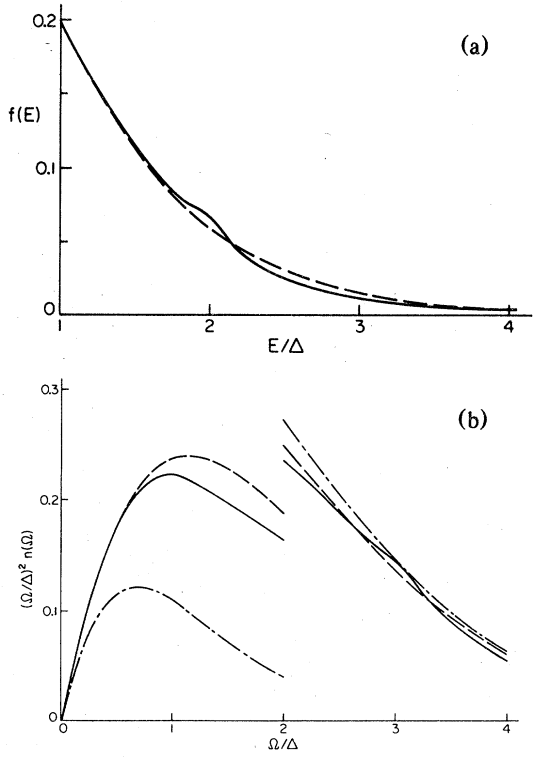

FIG. 1. (a) Solid curve is the quasiparticle distribution obtained from a numerical solution of the kinetic equations for $T_a=0.5\ T_c$, $\tau_{es}/\tau_0^{ph}=20$, $eV=2\Delta_0$, and $A=0.01$. The dashed curve is a Fermi distribution with $T^*=0.84\ T_c$. (b) Solid curve is a phonon spectrum obtained from the numerical solution. The dash-dot curve is Parker's T^* model, and the dashed curve is the extended T^* approximation given by Eq. (1).

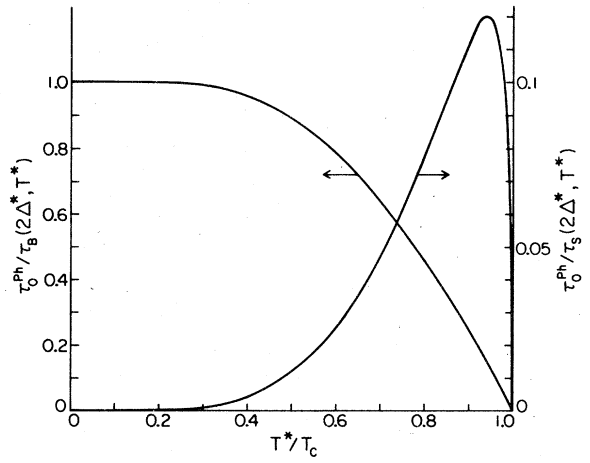

FIG. 2. Scattering and pair-breaking lifetimes of a phonon of energy $\Omega=2\Delta(T^*)$ vs T^*/T_c. Here τ_0^{ph} is the zero-temperature pair-breaking lifetime of a phonon of energy $2\Delta_0$.

solution both above and below 2Δ. The deviations reflect the fact that $f(E)$ is not strictly a Fermi function at temperature T^* as seen in Fig. 1(a).

A further simplification can be made without seriously degrading the approximate form for $n(\Omega)$ given by Eq. (1). This consists in replacing the frequency-dependent lifetimes $\tau_s(\Omega,T^*)$ and $\tau_B(\Omega,T^*)$ by their values for $\Omega=2\Delta(T^*)$. The integrals in Eq. (2) have been carried out for $\Omega=2\Delta(T^*)$ and the results versus T^*/T_c are shown in Fig. 2 and tabulated in Table I. Using this information it is then straightforward to determine an approximate $n(\Omega)$ distribution. For example, in the case just discussed $T^*=0.84\ T_c$, and from Fig. 2 we find that $\tau_0^{ph}/\tau_B(2\Delta(T^*),T^*)=0.40$ and $\tau_0^{ph}/\tau_s(2\Delta(T^*),T^*)=0.087$. Therefore, for $\tau_0^{ph}/\tau_{es}=0.05$ we have

$$n(\Omega)\cong\begin{cases}\dfrac{0.087n(\Omega,T^*)+0.05n(\Omega,T_a)}{0.087+0.05}, & 2\Delta>\Omega>0\ ,\\ \dfrac{(0.40+0.087)n(\Omega,T^*)+0.05n(\Omega,T_a)}{0.40+0.087+0.05}, & \Omega>2\Delta\ .\end{cases}\tag{3}$$

In Fig. 3 we compare the approximation for $n(\Omega)$ given by Eq. (3), dashed line, with $n(\Omega)$ given by Eq. (2), solid line, which contains the full frequency dependence of τ_s and τ_B. Clearly, little is lost by using the simpler form in which τ_s and τ_B are evaluated at $\Omega=2\Delta(T^*)$. In the following we shall use only this simpler form.

To get a further idea of the utility of the extended T^* model, we now examine some more cases. Basically we expect that our T^* description will be useful when $\tau_{es}\gg\tau_0^{ph}$. However, there is also the question of the signature of the drive. For example, tunnel injection has a strong signature compared, say, with

TABLE I. Pair-breaking and scattering lifetimes of a phonon of energy $2\Delta(T^*)$.

T^*/T_C	$\tau_0^{ph}/\tau_B(2\Delta^*,T^*)$	$\tau_0^{ph}/\tau_s(2\Delta^*,T^*)$
0.0	1.00	0
0.1	1.00	3.2×10^{-9}
0.2	1.00	3.1×10^{-5}
0.3	0.99	7.4×10^{-4}
0.4	0.96	4.0×10^{-3}
0.5	0.89	1.2×10^{-2}
0.6	0.79	2.6×10^{-2}
0.7	0.65	4.7×10^{-2}
0.8	0.46	7.7×10^{-2}
0.9	0.25	1.1×10^{-1}
0.98	0.052	1.0×10^{-1}

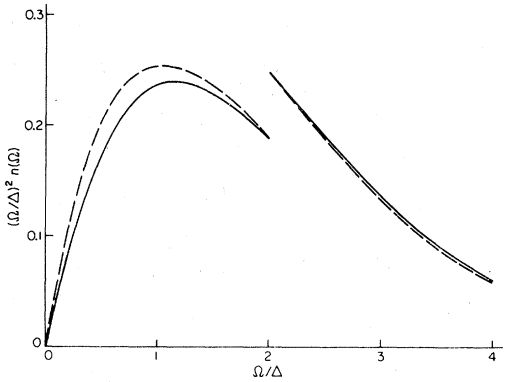

FIG. 3. Comparison of Eq. (3) (dashed curve) for $n(\Omega)$ with τ_s and τ_B evaluated at $\Omega=2\Delta(T^*)$ with Eq. (2) (solid curve) for $n(\Omega)$ with the full frequency dependence of τ_s and τ_B.

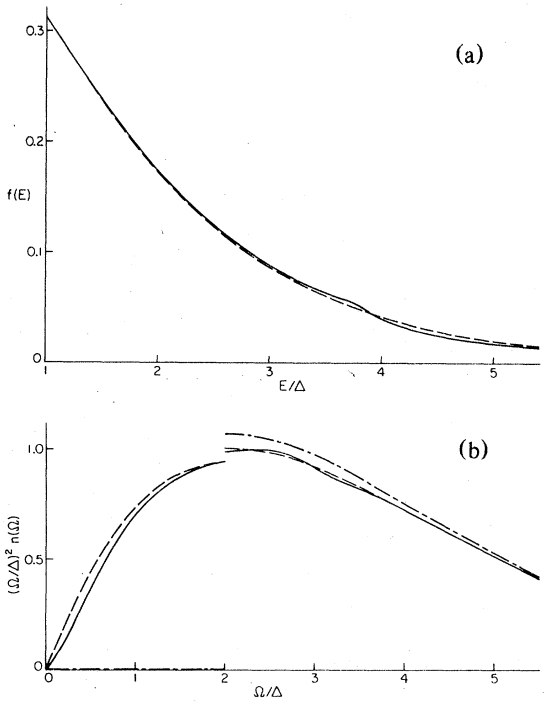

FIG. 4. (a) Solid curve is the quasiparticle distribution obtained from a numerical solution of the kinetic equations for $T_a=0$, $\tau_{es}/\tau_0^{ph}=60$, $eV=2\Delta_0$, and $A=0.01$. The dashed line is a Fermi distribution with $T^*=0.94\ T_c$. (b) Phonon spectrum with solid curve the numerical solution, the dash-dot curve Parker's T^* model, and the dashed curve our extended T^* model result with τ_s and τ_B evaluated at $2\Delta(T^*)$.

that produced in a heat or laser driven film because of the overlap of the density-of-states peaks when the bias voltage approaches $2\Delta/e$. For tunneling, with $eV \sim 2\Delta$, previously reported calculations[5] using the full kinetic equations have shown sharp structure in the driven quasiparticle and phonon distributions when $\tau_{es} \sim \tau_B$. Here we will continue to study the weakly thermal coupled case where $\tau_{es} >> \tau_B$.

In the following we consider several cases with $T_a = 0$ and the tunneling coupling fixed, as before, so that $A = 0.01$. We will look first at what happens if τ_{es}/τ_B is increased by a factor of 3 to 60 and the bias voltage is again taken as $2\Delta_0/e$. Figures 4(a) and 4(b) show $f(E)$ and $(\Omega/\Delta_0)^2 n(\Omega)$, respectively. The solid lines are the results obtained from solving the full nonlinear kinetic equations. The dashed curve is obtained from the extended T^* model using the simplified form in which τ_s and τ_B are set equal to their values at $2\Delta(T^*)$. The dash-dot lines in Fig. 4(b) show what one would obtain from Parker's T^* model which has $n(\Omega) = n(\Omega, T^*)$ for $\Omega > 2\Delta$ and $n(\Omega) = 0$ for $\Omega < 2\Delta$. Keeping all the parameters the same but decreasing τ_{es}/τ_0^{ph} to 20 we obtain the results shown in Figs. 5(a) and 5(b). Thus, as τ_{es}/τ_0^{ph} is decreased, deviations in the excitation distributions from our extended T^* model become apparent.

These deviations become larger when the bias voltage is decreased, but the tunneling coupling A remains fixed. In this case, approximately the same number of quasiparticles are injected into a narrower band of energies near the gap edge. In Figs. 6(a) and 6(b) we show results for $eV = 1.8\ \Delta_0$, $\tau_{es}/\tau_0^{ph} = 20$, and $T_a = 0$. Here the steady-state gap is $0.77\Delta_0$ so that eV is greater than 2Δ. In this case one sees pronounced deviations between the solutions of the kinetic equations and our T^* model results.

For tunneling injection we find that the steady-state quasiparticle and phonon distributions can be well described by the extended T^* model if the bias voltage is away from the gap edge and the phonon trapping factor is large. For other forms of the drive such as phonon injection via an external heat source or laser light where the initially generated excitations are more broadly distributed, the T^* distribution is even more closely approached for a given τ_{es}/τ_0^{ph} ratio.

For situations in which the T^* model is a good ap-

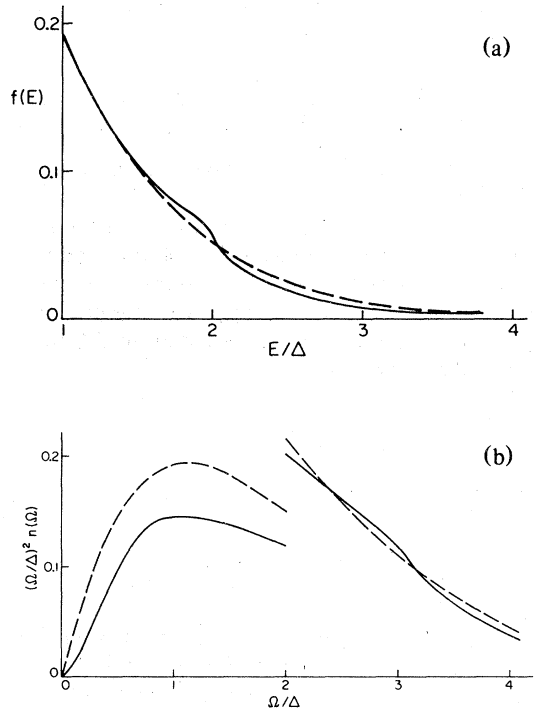

FIG. 5. (a) Quasiparticle distributions obtained from the numerical solution (solid) and the extended T^* model (dashed) for the same parameters as Fig. 4 except that τ_{es}/τ_0^{ph} is decreased to 20. The dashed curve has $T^* = 0.82\ T_c$. (b) Phonon spectra, numerical (solid) and extended T^* (dashed).

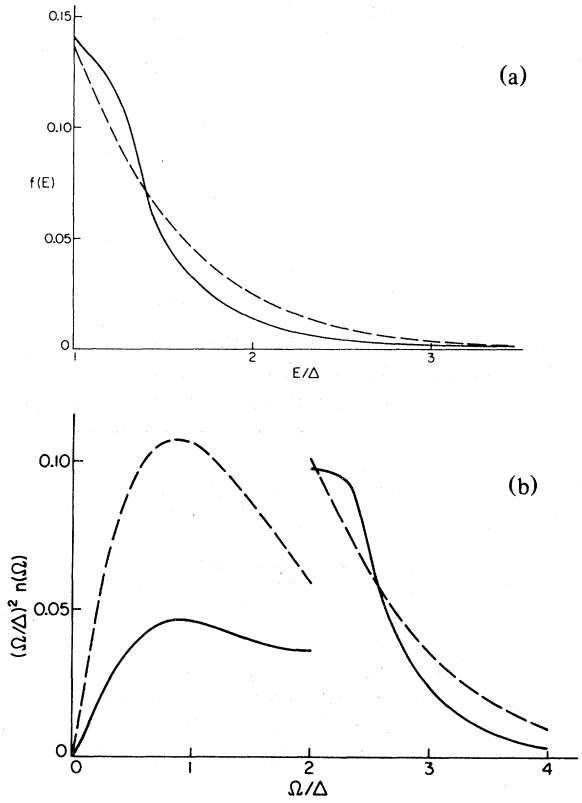

FIG. 6. (a) Quasiparticle distributions for a decreased bias voltage $eV = 1.8\ \Delta_0$ and $\tau_{es}/\tau_0 = 20$, $T_a = 0$, and $A = 0.01$. The dashed curve has $T^* = 0.75\ T_c$. (b) Phonon spectra, numerical (solid) and extended T^* (dashed).

proximation, it is useful to consider the relationship between the injected power and the steady-state gap Δ. This provides a way of predicting T^* and hence completes the T^* model since one no longer needs to measure Δ to get T^*. In steady state, the injected power P must be equal to the power emitted by phonons crossing the boundary. Therefore,

$$P=\frac{15C}{\pi^4\Delta_0^4}\int d\Omega\,\Omega^3[n(\Omega)-n(\Omega,T_a)] \ . \tag{4}$$

Here we have replaced the transmission coefficient for phonons near 2Δ by a constant and used the low-frequency phonon density-of-states form Ω^2. Taking $n(\Omega)$ equal to our extended T^* model form it is straightforward to express the integral in Eq. (4) in terms of the Debye-like energy function

$$g(x)=\frac{15}{\pi^4}\int_0^x dy\,y^3 n(y) \ . \tag{5}$$

We find that

$$\begin{aligned}\frac{P}{C}=&\frac{\tau_s^{-1}}{\tau_s^{-1}+\tau_{es}^{-1}}\frac{(kT^*)^4}{\Delta_0^4}g\left[\frac{2\Delta}{T^*}\right]\\&-\frac{\tau_s^{-1}}{\tau_s^{-1}+\tau_{es}^{-1}}\left[\frac{kT_a}{\Delta_0}\right]^4 g\left[\frac{2\Delta}{T_a}\right]\\&+\frac{\tau_s^{-1}+\tau_B^{-1}}{\tau_s^{-1}+\tau_B^{-1}+\tau_{es}^{-1}}\left[\frac{kT^*}{\Delta_0}\right]^4\left[1-g\left[\frac{2\Delta}{T^*}\right]\right]\\&-\frac{\tau_s^{-1}+\tau_B^{-1}}{\tau_s^{-1}+\tau_B^{-1}+\tau_{es}^{-1}}\left[\frac{kT_a}{\Delta_0}\right]^4\left[1-g\left[\frac{2\Delta}{T_a}\right]\right] \ ,\end{aligned} \tag{6}$$

with

$$\tau_s^{-1}=\tau_s^{-1}(2\Delta,T^*) \ , \quad \tau_B^{-1}=\tau_B^{-1}(2\Delta,T^*)$$

given in Fig. 3, and $\Delta=\Delta(T^*)$ determined from the BCS relation. Thus Eq. (6) is an implicit relation for Δ or T^* in terms of the drive power P. For $T_a=0$,

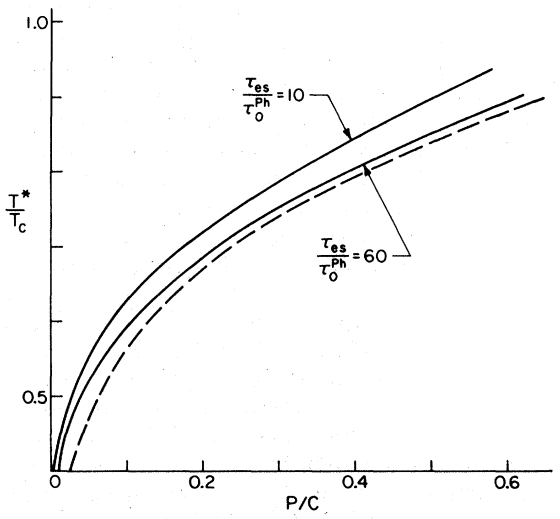

FIG. 7. Plots of T^*/T_c vs P/C for $T_a=0$ and $\tau_{es}/\tau_0^{ph}=10$ and 60. The dashed curve corresponds to simple heating, Eq. (7).

we have plotted T^*/T_c vs P/C in Fig. 7 for $\tau_{es}/\tau_0^{ph}=10$ and 60. Note that if the film was simply heated to a temperature T^* so that $n(\Omega)=n(\Omega,T^*)$, we would have

$$\frac{P}{C}=\left[\frac{kT^*}{\Delta_0}\right]^4-\left[\frac{kT_a}{\Delta_0}\right]^4 \ . \tag{7}$$

This equation with $T_a=0$ is shown in Fig. 7 as the dashed curve.

To summarize, if $\tau_{es}\gg\tau_0^{ph}$ as is often the situation, we find that the quasiparticle and phonon distributions can be described by an extension of the Parker T^* model. Here the quasiparticles are determined by a Fermi distribution at a temperature T^*, and the phonons are given by

$$n(\Omega)=\begin{cases}\dfrac{\tau_s^{-1}n(\Omega,T^*)+\tau_{es}^{-1}n(\Omega,T_a)}{\tau_s^{-1}+\tau_{es}^{-1}} \ , & 2\Delta>\Omega>0 \ ,\\ \dfrac{(\tau_s^{-1}+\tau_B^{-1})n(\Omega,T^*)+\tau_{es}^{-1}n(\Omega,T_a)}{\tau_s^{-1}+\tau_B^{-1}+\tau_{es}^{-1}} \ , & \Omega>2\Delta \ .\end{cases} \tag{8}$$

The lifetimes τ_s and τ_B are evaluated at $\Omega=2\Delta$, with Δ the BCS gap for a temperature T^*. If the thermal coupling parameter τ_{es}/τ_0^{ph} and the drive level P/C are known, Eq. (6) can be used to determine $\Delta(T^*)$ and hence T^*. Alternatively, if the nonequilibrium steady-state value of Δ is known, it can be used to determine T^*. Then τ_s and τ_B can be found from Fig. 2 or Table I and used in Eq. (8) to specify $n(\Omega)$.

ACKNOWLEDGMENTS

D. J. Scalapino would like to acknowledge ONR for research support. W. Y. Lai is partly supported by NSF Grant No. PHY 76-81713, and Jhy-Jiun Chang is partly supported by NSF Grant No. DMR 78-17813.

[1]J. J. Chang and D. J. Scalapino, J. Low Temp. Phys. 31, 1 (1978).
[2]W. H. Parker, Phys. Rev. B 12, 3667 (1975).
[3]S. B. Kaplan, C. C. Chi, D. N. Langenberg, J. J. Chang, S. Jafarey, and D. J. Scalapino, Phys. Rev. B 14, 4854 (1976).

[4]Parameter $A=(\sigma_N\tau_0 T_c^3)/2N(0)e^2 d\Delta_0^3$ is a measure of the strength of the current injection. Here σ_N is the normal junction conductance per unit area, τ_0 is the characteristic quasiparticle lifetime (see Ref. 3), $N(0)$ is the single-spin Bloch density of states at the Fermi surface, and d is the film thickness. For an Al film thickness 500 Å, $A=0.01$ corresponds to a current density of approximately 5 A/cm^2.

[5]If $f(E)=f(E,T_a\mu^*)=\{\exp[(E-\mu^*)/kT_a]+1\}^{-1}$, the steady-state phonon spectrum calculated from the kinetic equation would be

$$n(\Omega)=\begin{cases} n(\Omega,T_a), & \Omega<2\Delta, \\ \dfrac{n(\Omega,T_a)[\tau_s^{-1}(\Omega,\mu^*)+\tau_{es}^{-1}]+n(\Omega,T_a,2\mu^*)\tau_B^{-1}(\Omega,\mu^*)}{\tau_s^{-1}(\Omega,\mu^*)+\tau_{es}^{-1}+\tau_B^{-1}(\Omega,\mu^*)}, & \Omega>2\Delta. \end{cases}$$

Here $\tau_s^{-1}(\Omega,\mu^*)$ and $\tau_B^{-1}(\Omega,\mu^*)$ are given by Eqs. (2a) and (2b), respectively, with $f(E,T^*)$ replaced by $f(E,T_a,\mu^*)$ and $n(\Omega,T_a,2\mu^*)=\{\exp[(\Omega-2\mu^*)/kT_a]-1\}^{-1}$. Note that, contrary to the numerical solution of the kinetic equations, the form for $n(\Omega)$ predicted using this μ^* Fermi distribution is equal to $n(\Omega,T_a)$ for $\Omega<2\Delta$.